Histol Histopathol (2023) 38: 893-905

http://www.hh.um.es

Histology and Histopathology
From Cell Biology to Tissue Engineering

ORIGINAL ARTICLE **Open Access**

Circ_0008234 regulates the biological process of gallbladder carcinoma by targeting the miR-204-5p/FGFR2 axis

Na Zhang[1]*, Jing Li[2]*, Huapeng Sun[3], Aixia Tian[4] and Yuhua Chen[1]

[1]Department of Pathology, [2]Department of Oncology, [3]Department of General Surgery and [4]Department of Gastroenterolgy, Xiangyang Central Hospital, Affiliated Hospital of Hubei University of Arts and Science, Xiangyang, Hubei, China

*Na Zhang and Jing Li contributed to this work equally as co-first authors

Summary. Background. Gallbladder carcinoma (GBC) is a common cancer disease with high mortality. Circular RNA_0008234 (circ_0008234) has been shown to play a key role in many tumors, including GBC. However, the function between circ_0008234 and microRNA-204-5p (miR-204-5p) in the progression of GBC has not been clarified.

Methods. Quantitative real-time polymerase chain reaction (qRT-PCR) was used to detect the expressions of circ_0008234, miR-204-5p and fibroblast growth factor receptor-2 (FGFR2) in GBC cells and tissues. Western blot was used to detect the expression of relative proteins. Cell proliferation, apoptosis, invasion and migration were detected by 3-(4, 5-dimethylthiazol-2-yl)-2, 5-diphenyltetrazolium bromide (MTT) assay, thymidine analog 5-ethynyl-2'-deoxyuridine (EdU) assay, flow cytometry, transwell assay and wound healing assay. Mechanically, the interaction of miR-204-5p with circ_0008234/FGFR2 was notarized by dual-luciferase reporter assay. A xenotransplantation model was established to study the role of circ_0008234 *in vivo*.

Results. Circ_0008234 and FGFR2 were highly expressed in GBC tissues and cells. Silencing circ_0008234 down-regulated cell proliferation, migration and invasion of NOZ and SGC-996 cells, while miR-204-5p inhibitors reversed these effects. In addition, overexpression of FGFR2 restored the cell malignant behavior of GBC cells inhibited by miR-204-5p mimic. Animal experiments confirmed the anti-tumor effect of silenced circ_0008234 *in vivo*.

Conclusion: Circ_0008234 mediated GBC via the miR-204-5p/FGFR2 axis, providing a novel targeted therapy for gallbladder carcinoma.

Key words: Circ_0008234, miR-204-5p, FGFR2, Gallbladder carcinoma

Corresponding Author: Aixia Tian, MM. Department of Gastroenterolgy, Xiangyang Central Hospital, Affiliated Hospital of Hubei University of Arts and Science, No.136, Jingzhou Street, Xiangyang City, Hubei Province, 441021 Hubei, China. e-mail: Tianaixia016@163.com

DOI: 10.14670/HH-18-538

Introduction

Gallbladder cancer (GBC) is the most common type of biliary tract cancer, malignant tumor originating from the gallbladder epithelium (Hickman and Contreras, 2019). Because of its aggressiveness, it is prone to metastasis to regional lymph nodes (Fong et al., 2000). Due to the lack of specific signs and diagnostic markers for early GBC, most patients with GBC are not diagnosed until the middle and late stages, and results in a five-year survival rate of only 10-25% for GBC (Konstantinidis et al., 2009; Sharma et al., 2017). Currently, the only treatment for GBC is complete surgical resection, but the prognosis is poor (Krell and Wei, 2019). Therefore, understanding the molecular mechanism of GBC pathogenesis and finding biomarkers for early diagnosis are crucial.

Circular RNAs (circRNAs), without 5'cap and 3'tail structure, are circular non-coding RNAs (Danan et al., 2012; Liu et al., 2017; Zhang et al., 2018). In recent years, many studies have been conducted on the relationship between circRNAs and cancer. However, there are few studies on circRNAs and GBC. For example, Wang et al. discovered that circ_MTO1 expression is significantly up-regulated in GBC patients, and abnormal circ-MTO1 expression can be used as a prognostic factor of GBC (Wang et al., 2020). Similarly, circ_FOXP1 (circ_0008234) was increased in GBC patients, regulating GBC cell behavior (Wang et al., 2019). However, it has not been reported whether circ_0008234 plays a role in GBC as a competitive endogenous RNA (ceRNA) or sponge for microRNA (miRNA).

MicroRNAs (miRNAs) are 22 nucleotide non-coding RNA that negatively regulate target genes by interacting with 3'untranslated regions (3'UTR) (Krol et al., 2010; Melo and Esteller, 2014). Many studies have reported the regulatory impact of miRNA in GBC. For example, miR-145, miR-31 and miR-433 can regulate GBC progression and chemotherapy resistance (Li et al., 2016; Zhan et al., 2016; Yu et al., 2018). Similarly, miR-204 was lowly expressed in GBC patients, and can be used as a diagnostic indicator (Zhang et al., 2021). And we predicted that fibroblast growth factor receptor-2 (FGFR2) was a direct target of miR-204-5p. Studies have shown that FGFR2 plays a role as an oncogenic factor in various cancers, such as colorectal cancer, breast cancer, pancreatic cancer and cholangiocarcinoma (Narong and Leelawat, 2011; Czaplinska et al., 2016; Li et al., 2019, 2020). However, whether FGFR2 is regulated by miR-204-5p in GBC has not been investigated.

Here, we investigated the impact of circ_0008234 in GBC by silencing circ_0008234 in GBC cell lines. Moreover, the effect of the circ_0008234/ miR-204-5p / FGFR2 axis on GBC cells was explored. The results showed that circ_0008234 may be a new biomarker for GBC.

Materials and methods

Clinical tissue samples

Tumor tissues and the adjacent non-tumor gallblader tissue samples from 29 GBC patients who underwent surgical resection in Xiangyang Central Hospital, Affiliated Hospital of Hubei University of Arts and Science were collected. Subsequently, the samples were frozen and preserved at -80°C for use. None of the patients received any treatment before surgery, and their clinicopathologic features are presented in Table 1. Patients with other tumors, digestion system diseases, cardiovascular diseases, diabetes, or infections were excluded from this study. All patients have written informed consent. The study was audited by Xiangyang Central Hospital, Affiliated Hospital of Hubei University of Arts and Science.

Cell lines and cell culture

Human intrahepatic biliary epithelial cell line H69 and Human GBC cell lines (GBC-SD, QBC939, NOZ and SGC-996) were obtained from ATCC (Manassas, VA, USA). All cells were conventionally cultured in RPMI-16 medium in an incubator containing 5% CO_2 at 37°C.

Cell Transfection

The following plasmids were synthesized by Ribobio Co., Ltd. (Guangzhou, China): si-circ_0008234 and si-NC, overexpressed circ_0008234 vector (circ_0008234) and pCD5-ciR, miR-204-5p inhibitor (anti-miR-204-5p) and anti-miR-NC, miR-204-5p mimic (miR-204-5p) and miR-NC, FGFR2 overexpression vector (FGFR2) and pcDNA, and transfected into GBC cells according to Lipofectamine 2000 (Thermo Fisher) specifications.

Histopathological examination

The excised fresh tissue was fixed with 4% paraformaldehyde, dehydrated in alcohol and embedded in paraffin. The sections were then stained with hematoxylin and eosin (H&E). Sections were examined by light microscopy and pictures were obtained using a DSC-L1 Nikon Imaging System.

Immunohistochemical (IHC) staining analysis

The excised fresh tissue was fixed with 4% paraformaldehyde, dehydrated in alcohol and embedded in paraffin. Paraffin sections (5 μM) were dewaxed and rehydrated for antigen stripping. Membranes were incubated with anti-Ki-67 (1:200, ab15580; Abcam), anti-FGFR2 (1:100, ab235377, Abcam) and anti-MMP9 (1:100, ab76003, Abcam) at 4°C overnight, and then incubated with the Goat against mouse IgG (1:10,000, ab205719, Abcam) 1h. Sections were stained with diaminobenzidine (DAB) kit (Sigma, St Louis, MO, USA) according to protocol. The positive staining was observed with a light microscope.

Quantitative real-time polymerase chain reaction (qRT-PCR)

Total RNA was extracted from normal tissues and cells and GBC tissues and cells using Trizol reagent (Thermo Fisher), cDNA was synthesized using reverse transcription kit (Thermo Fisher), and qRT-PCR was

Table 1. Relationship between circ_0008234 expression and the clinicopathologic features of gallbladder carcinoma patients (n=29).

Characteristics		circ_0008234 expression		P value
	n=29	Low(n=14)	High(n=15)	
Age (years)				0.7104
≤50	12	5	7	
>50	17	9	8	
TNM grade				0.0092*
I+II	13	10	3	
III-IV	16	4	12	
Lymph node metastasis				0.0078*
Positive	18	5	13	
Negative	11	9	2	
Tumor size				0.0268*
≤5 cm	14	10	4	
>5 cm	15	4	11	

TNM, tumor-node-metastasis; *P<0.05 by chi-square test.

performed using SYBR Green qRT-PCR Mix (Takara, Shiga, Japan). β-actin and U6 were used as controls to calculate relative expression levels by the $2^{-\Delta\Delta Ct}$ method. All the primers are listed in Table 2.

Western blot analysis

Protein extraction reagent and BCA protein quantification reagent were used for protein extraction and quantification respectively. The proteins were isolated by 12% SDS-PAGE and transferred to PVDF membrane. After plugging the membrane with 5% skim milk, the antibodies of β-actin (1:1,000, ab8226, Abcam, Cambridge, MA, USA), CyclinD1 (1:1,000, ab40754, Abcam), MMP9 (1:1,000, ab76003, Abcam), and FGFR2 (1:1,000, ab109372, Abcam) were incubated respectively. Lastly, the protein was visualized using Clarity™ Western ECL Substrate Kit (Bio-Rad, Shanghai, China).

CircRNA validation

Total RNA (3 μg) extracted from GBC cells was added with RNase R (3 U/μg, Epicentre Technologies, Madison, WI, USA) and incubated at 37°C for 30 min. The corresponding expressions of circ_0008234 and FOXP1 were detected by qRT-PCR.

Cellular distribution analysis

The nucleus and cytoplasm of GBC cells were isolated according to Paris kits (Life Te-Technologies, CA, USA) instructions. Then, cytoplasmic and nuclear RNA was isolated using Trizol reagent. Using GAPDH and U6 as controls, the expression of circ_0008234 in cytoplasmic or nuclear parts was detected by qRT-PCR.

3-(4, 5-dimethylthiazol-2-yl)-2, 5-diphenyltetrazolium Bromide (MTT) assay

GBC cells transfected for 48h were inoculated into 96-well plates at a density of 2×10^3 cells/well. After 48h of routine incubation, 20 μL MTT solution was added to each well. After 2h of incubation, 150 μL DMSO was added to dissolve formazan by low-speed shock. The absorbance of each well was measured at 570 nm with a microplate reader.

Table 2. Sequences of primers used for PCR.

Name		Primers for PCR (5'-3')
hsa_circ_0008234	Forward	CTCTGCACCTTCCAAGACCT
	Reverse	GTGCATTTGCTGGGGAGTGATA
FOXP1	Forward	CTTACTAGAGTGCGGCGGTC
	Reverse	GCAGGACTTCCAACTCCCAA
miR-107	Forward	GCCGAGTTCCCTTTGTCACCT
	Reverse	CAGTGCGTGTCGTGGAGT
FGFR2	Forward	CCTGCGGAGACAGGTAACAG
	Reverse	GGTGTCTGCCGTTGAAGAGA
β-actin	Forward	CTCGCCTTTGCCGATCC
	Reverse	GGGGTACTTCAGGGTGAGGA
U6	Forward	CTCGCTTCGGCAGCACA
	Reverse	AACGCTTCACGAATTTGCGT

Thymidine analog 5-ethynyl-2'-deoxyuridine (EdU) assay

Apollo dye was prepared according to the instructions of the Cell-Light EdU DNA Cell Proliferation Kit (RiboBio), and the transfected GBC cells were stained for 30 min under dark conditions, and the nuclei were stained with Hoechst 33,342. Five fields were randomly selected for observation under the microscope.

Transwell invasion assays

The transfected GBC cells were suspended in serum-free medium and prepared as 1×10^6/mL cell suspension. 200 μL cell suspension was added to the upper chamber of transwell chamber (BD Biosciences, San Diego, CA, USA), while 500 μL culture medium containing 10% FBS was added to the lower chamber of the 24-well plate. After 24h of incubation in a 37°C incubator, the cells on the lower chambers were fixed with 4% paraformaldehyde and stained with 0.5% crystal violet. Three fields were randomly selected under the microscope to observe and count.

Wound-healing analysis

The transfected GBC cells were prepared in cell suspension with a density of 1×10^3 cells/mL, and 500 μL was added into the 6-well plate overnight to form monolayer cells. A horizontal line was drawn on the surface of monolayer cells with the tip of 10 μL pipetting gun, and the cells were washed with PBS 3 times to remove the scratched and detached cells. The initial scratch width was measured by photographing under a microscope. After incubation for 24h in an incubator containing 5% CO_2 at 37°C, the width of scratches was measured again.

Flow cytometry assay

GBC cells were washed with PBS, collected and suspended in 200 μL binding buffer containing 10 μL Annexin-FITC (BD Biosciences), and incubated for 30 min at room temperature without light. 5 μL PI and 300 μL binding buffer were added, and the apoptosis rate of each group was detected by flow cytometry after mixing.

Dual-luciferase reporter assay

Wild type (WT) or mutant type (MUT) sequences of circ_0008234 or FGFR2 3'UTR containing miR-204-5p binding sites were cloned into pmirGLO vectors to form

wild-type luciferase reporter plasmids WT-circ_0008234 and FGFR2 3'UTR-WT and mutated luciferase reporter plasmids MUT-circ_0008234 and FGFR2 3'UTR-MUT. Corresponding reporter plasmids were co-transfected into GBC cells with miR-204-5p mimics or miR-NC, respectively. Dual-Luciferase Reporter Assay Kit (GeneCopoeia, Rockville, MD, USA) was used to analyze the firefly luciferase and sea kidney luciferase activities of GBC cells 48h after transfection, and the ratio of the two was used to represent the relative luciferase activities.

Xenograft models

All animal experiments were approved by Xiangyang Central Hospital, Affiliated Hospital of Hubei University of Arts and Science Animal Care and Use Committee. Ten 8-week-old male BALB/c nude mice were purchased from Weidahe Laboratory Animal Science and Technology Co., Ltd. (Beijing, China) and randomly divided into 2 groups (sh-NC group and sh-circ_0008234 group) with 5 mice in each group. SGC-996 cells transfected with sh-NC or sh-circ_0008234 were subcutaneously injected to establish tumor xenograft tumor. After one week, the tumor size was measured every 3 days and the tumor volume was calculated using the following formula: volume =1/2 (length×width^2). After 22 days, the mice were sacrificed by neck amputation and the tumor was taken out and weighed.

Statistical analysis

Three replicates were set for each experimental group, and results were expressed as mean ± standard deviation (SD). GraphPad Prism 7 software was used for statistical analysis, Student's t-test was used to compare differences between two groups, and one-way ANOVA was used to compare differences between multiple groups. $P<0.05$ was statistically significant difference.

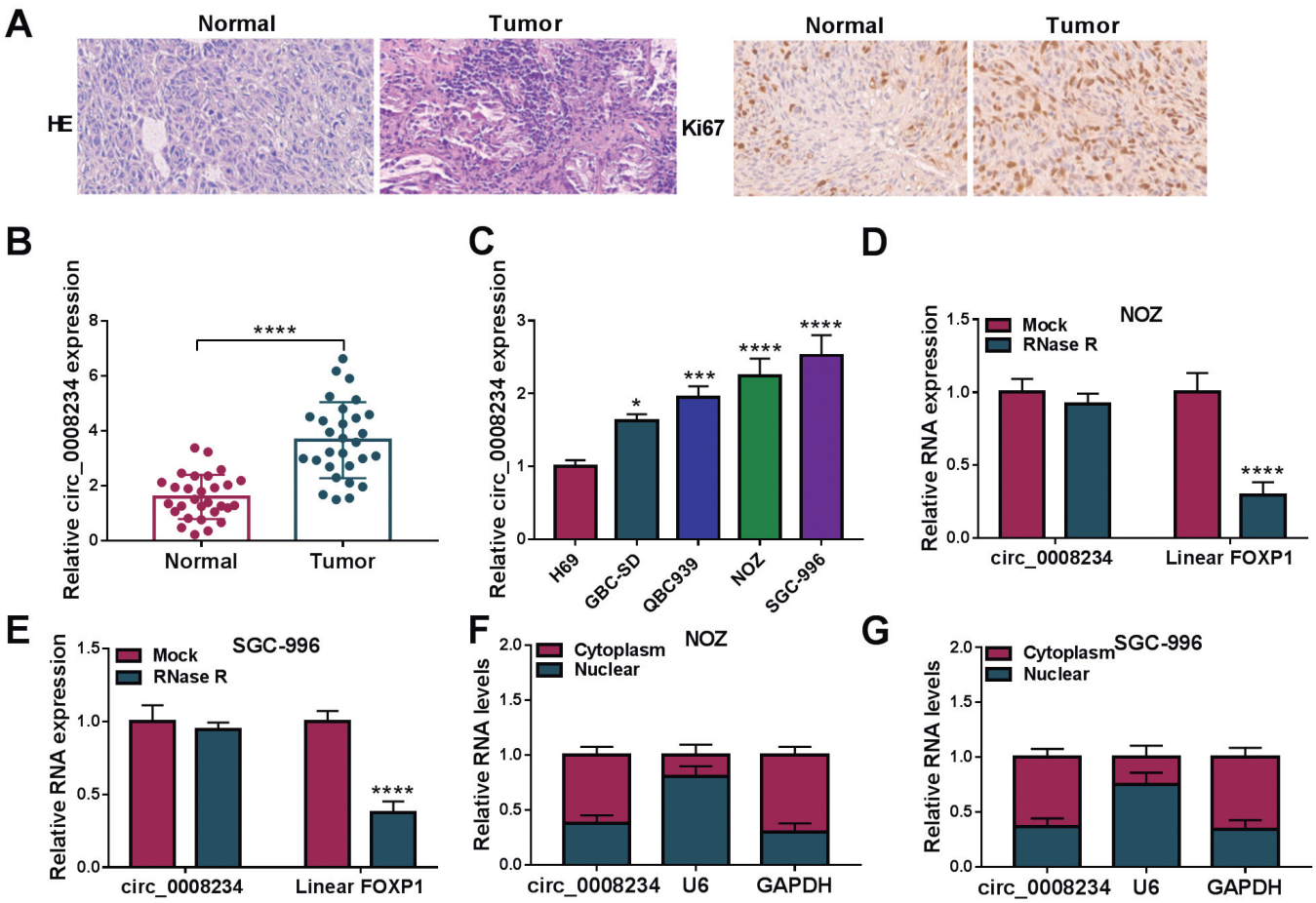

Fig. 1. Circ_0008234 was highly expressed in GBC tissues and cell lines. **A.** The pathological sections of the tumor tissue and normal tissue of patients with GBC, and the positive rate of Ki67 was analyzed by IHC. **B, C.** The expression of circ_0008234 in GBC tissues (n=29) and cell lines was tested by qRT-PCR. **D, E.** The relative RNA levels of circ_0008234 and FOXP1 in NOZ and SGC-996 cells were analyzed by qRT-PCR after RNase R treatment. **F, G.** The distribution of circ_0008234 in nucleus or cytoplasm was determined by qRT-PCR. **P*<0.05, ***P*<0.01, ****P*<0.001, *****P*<0.0001.

Results

Circ_0008234 was up-regulated in GBC tissues and cell lines

Firstly, we validated the pathological changes of GBC tumors by H&E staining. Tumor tissues have stronger proliferation ability than normal tissues. To validate the enhanced growth of tumor tissues, we perform IHC assay by staining for cell proliferation using the cell-cycle marker Ki67. The results showed that the positive rate of Ki67 was notably increased in GBC tumor tissues (Fig. 1A). Then, in order to investigate the role of circ_0008234 in gallbladder carcinoma, we detected the expression level of circ_0008234 in GBC tissues by qRT-PCR. The results showed that the expression of circ_0008234 was significantly increased in GBC tissues (n=29) compared to normal tissues (n=29) (Fig. 1B). Meanwhile, it was found that compared with H69 cells, the expression of circ_0008234 was significantly increased in GBC cells, and circ_0008234 was better expressed in NOZ and SGC-996, so NOZ and SGC-996 were selected in subsequent experiments (Fig. 1C). Furthermore, circ_0008234 is resistant to RNase R, indicating that circ_0008234 is circular (Fig. 1D,E). Finally, we isolated RNA samples from the cytoplasm and nucleus of NOZ and SGC-996 cells and found that circ_0008234 was mainly distributed in the cytoplasm relative to the nucleus (Fig. 1F,G). Additionally, circ_0008234

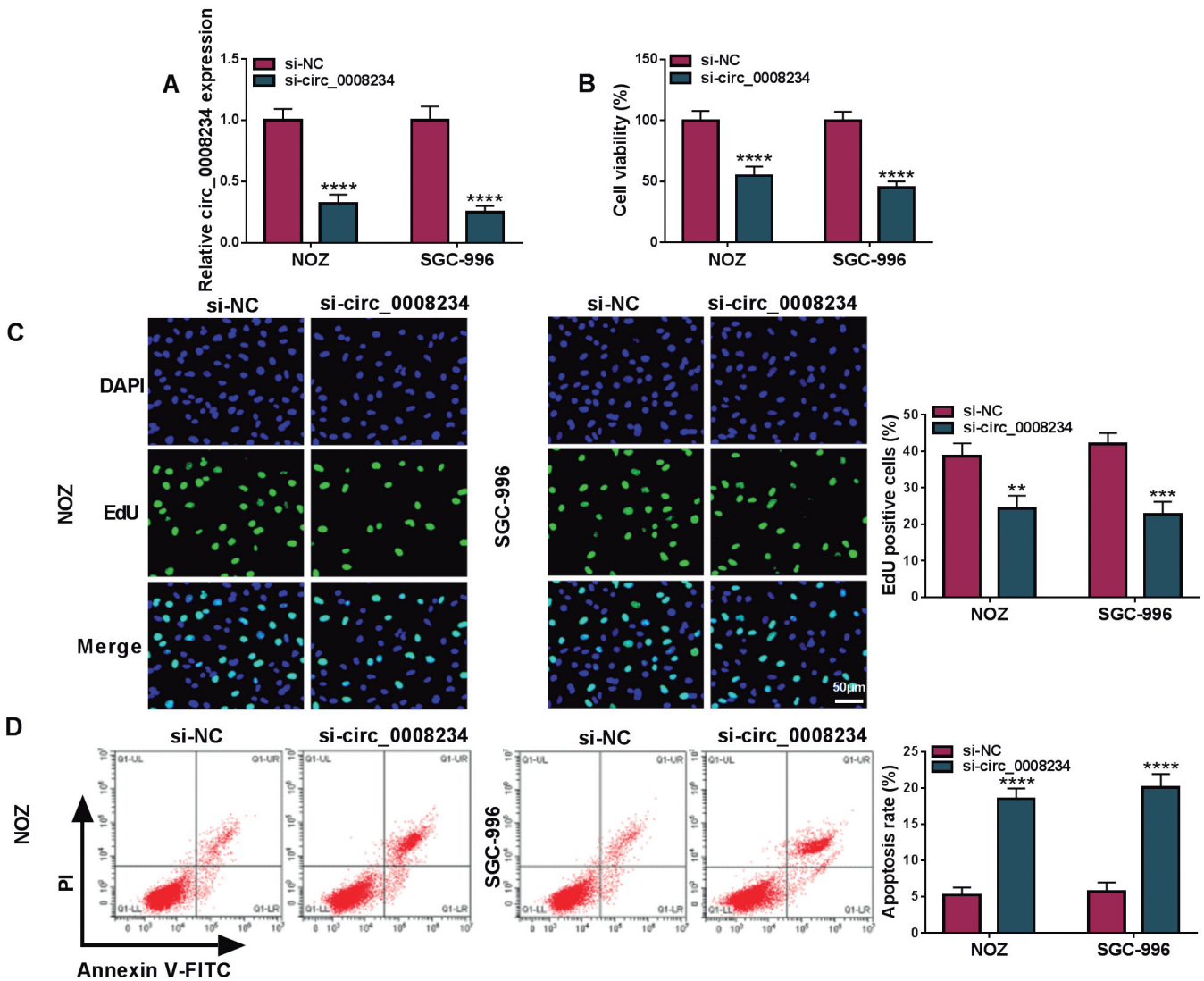

Fig. 2. Si-circ_0008234 reduced cell proliferation and induced cell apoptosis migration and invasion. **A.** The knockdown efficiency of circ_0008234 was determined by qRT-PCR. **B.** MTT detected the cell viability. **C.** EdU assay was used to assess EdU positive cells. **D.** Cell apoptosis detected by flow cytometry. ***P*<0.01, ****P*<0.001, *****P*<0.0001.

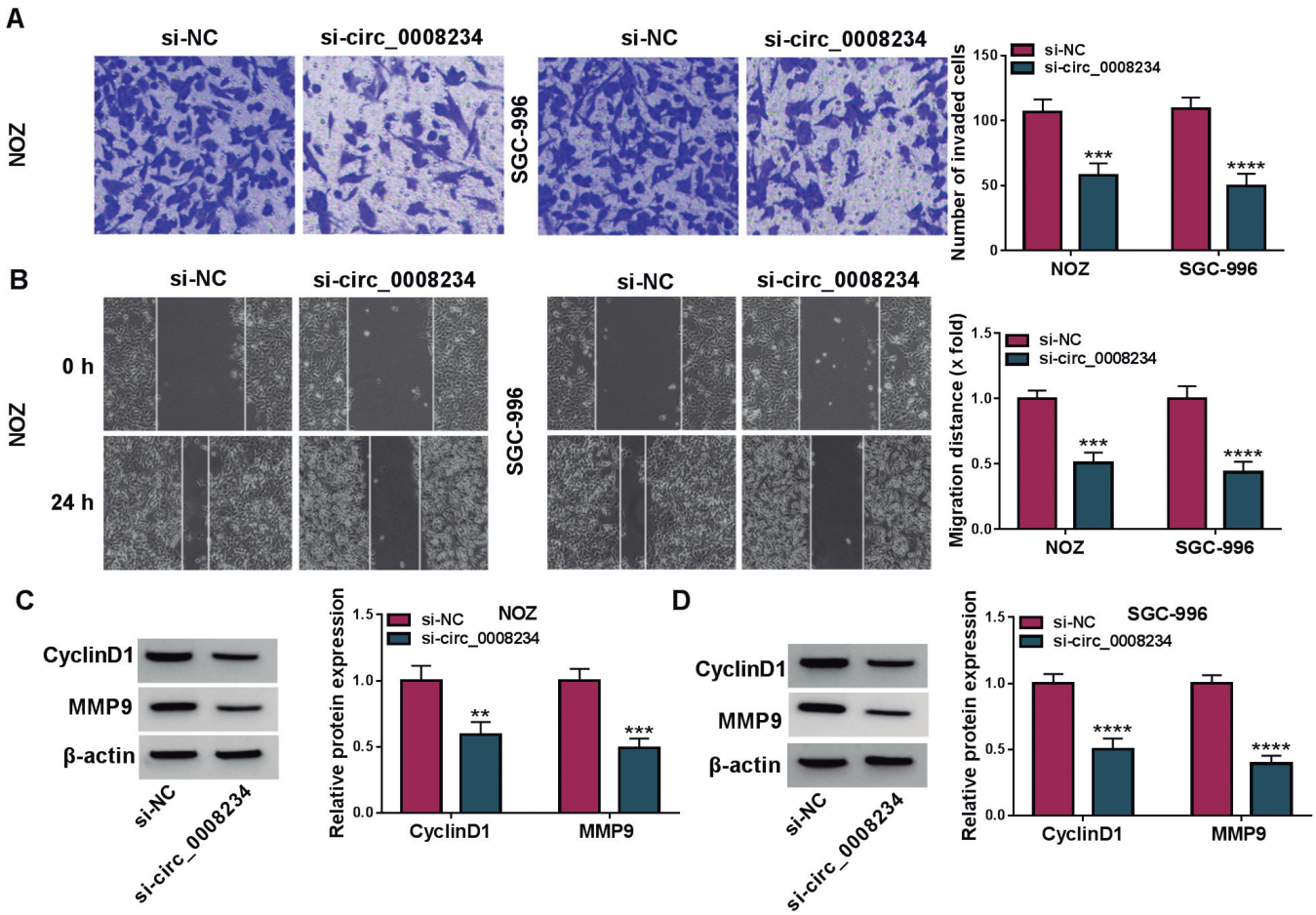

Fig. 3. Si-circ_0008234 reduced cell migration and invasion. **A.** Transwell detected cell invasion ability. **B.** Wound healing assay was used to examine cell migration ability. **C, D.** Western blot assay was used to test the relative protein level. ***P*<0.01, ****P*<0.001, *****P*<0.0001.

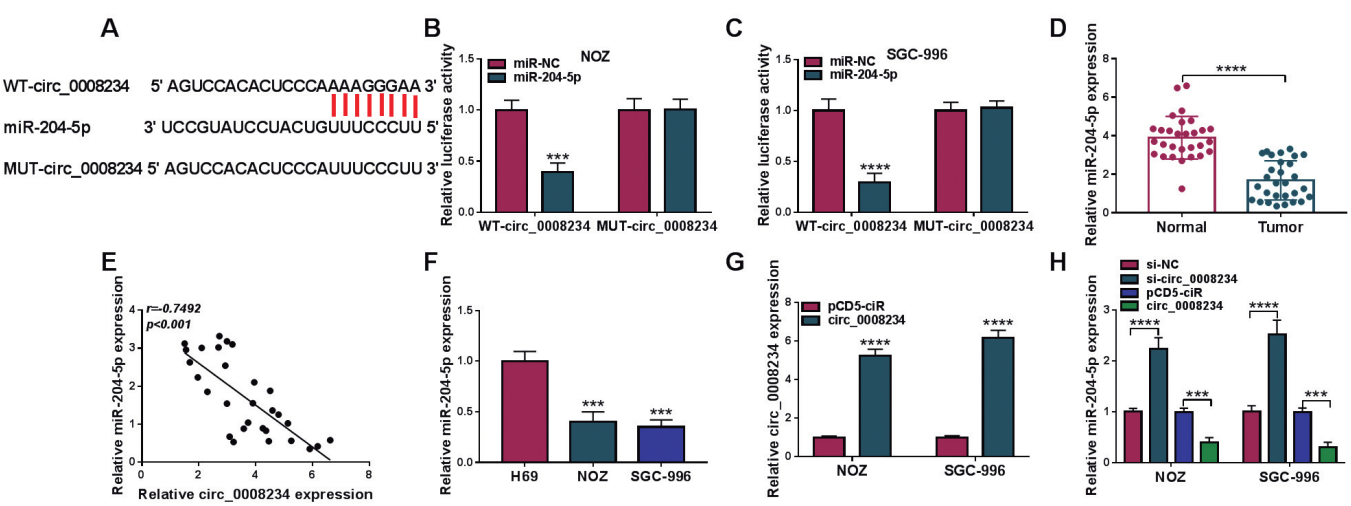

Fig. 4. MiR-204-5p binds to circ_0008234. **A.** Starbase predicted the binding sites of circ_0008234 to miR-204-5p. **B, C.** Dual-luciferase reporter assays were performed to confirm the association between circ_0008234 and miR-204-5p. **H, I.** PIR assay detected the combination of circ_0008234 and miR-204-5p. **D, F.** The expression of miR-204-5p in GBC tissues (n=30) and cells was tested by qRT-PCR. **E.** The correlation between circ_0008234 and miR-204-5p was analyzed by Pearson's correlation analysis. **G, H.** QRT-PCR detected the expression of circ_0008234 and miR-204-5p. ****P*<0.001, *****P*<0.0001.

expression was closely associated with the TNM stage, lymph node metastasis and tumor size of these tumor samples from GBC patients (Table 1). Taken together, these data suggest that circ_0008234 is significantly up-regulated in GBC tissues and cell lines.

Knockdown of circ_0008234 inhibited the malignant behavior of GBC cells.

The qRT-PCR results showed that circ_0008234 expression was significantly down-regulated in NOZ and SGC-996 cells after siRNA to circ_0008234 transfection (Fig. 2A). As shown in Fig. 2B, MTT results showed that the cell viability of NOZ and SGC-996 cells was significantly decreased by knockdown of circ_0008234. And when circ_0008234 was knocked down, the rate of EdU positive cells of NOZ and SGC-996 cells was significantly reduced (Fig. 2C). Moreover, silencing circ_0008234 increased the apoptosis rate of NOZ and SGC-996 cells (Fig. 2D). Similarly, compared with si-NC control, NOZ and SGC-996 cells transfected with si-circ_0008234 showed significantly reduced invasion ability (Fig. 3A). Also, wound healing assay showed that silencing circ_0008234 notably reduced the migration ability in NOZ and SGC-996 cells (Fig. 3B). Lastly, western blot results showed that the protein levels of CyclinD1 and MMP9 were significantly decreased by si-circ_0008234 (Fig. 3C,D). Taken together, these findings suggest that circ_0008234 knockdown inhibited the malignant behavior of GBC cells.

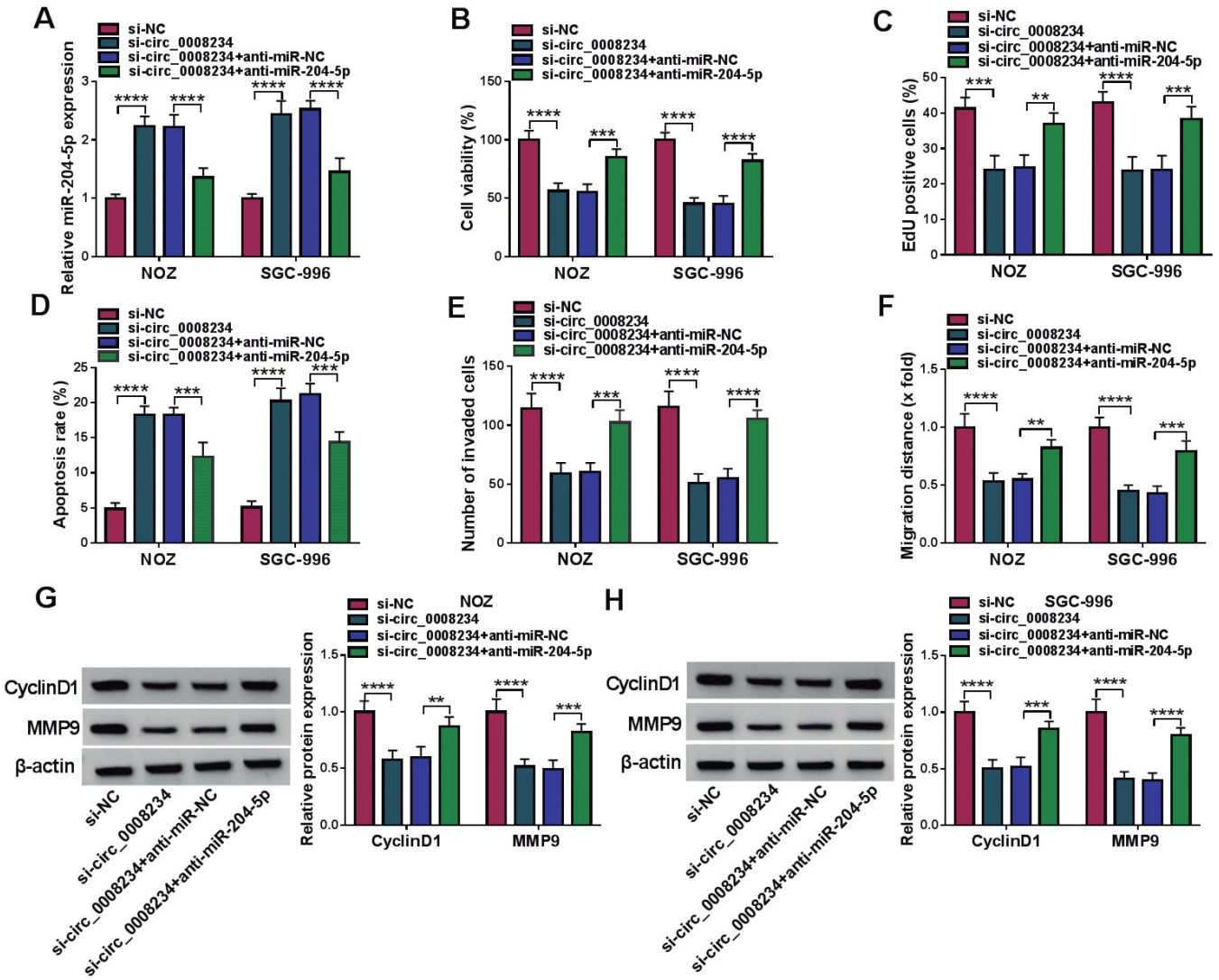

Fig. 5. Anti-miR-204-5p restored cell proliferation, migration, and invasion reduced by si-circ_0008234. **A.** The expression of miR-204-5p was determined by qRT-PCR. **B.** MTT detected the cell viability. **C.** EdU assay was used to assess EdU positive cells. **D.** Cell apoptosis detected by flow cytometry. **E.** Transwell detected cell invasion ability. **F.** Wound healing assay was used to examine cell migration ability. **G, H.** Western blot assay was used to test the relative protein level. ***P*<0.01, ****P*<0.001, *****P*<0.0001.

Anti-miR-204-5p restored the effect of si-circ_0008234 on GBC cells

Starbase (http://starbase.sysu.edu.cn/agoClipRNA.php?source=mRNA) predicted that circ_0008234 had a binding site with miR-204-5p (Fig. 4A). The results of dual luciferase reporter assay showed that the luciferase activity of the reporter gene vector WT-circ_0008234 was significantly lower than that of the control group in NOZ and SGC-996 cells transfected with miR-204-5p, while the luciferase activity of MUT-circ_0008234 was not changed (Fig. 4B,C). Next, the results of qRT-PCR detection showed that the expression of miR-204-5p was significantly reduced in gallbladder carcinoma tissues (Fig. 4D). Pearson's correlation analysis showed that miR-204-5p was negatively regulated with circ_0008234 (Fig. 4E). Similarly, the expression of miR-204-5p was remarkably abolished in NOZ and SFC-996 cells (Fig. 4F). The overexpressed efficiency of circ_0008234 was detected by qRT-PCR (Fig. 4G). In addition, silenced circ_0008234 up-regulated the expression of miR-204-5p, while overexpressed circ_0008234 inhibited the expression of miR-204-5p (Fig. 4H). To sum up, miR-204-5p was a target of circ_0008234.

Silenced circ_0008234 up-regulated the expression of miR-204-5p, while anti-miR-204-5p decreased it (Fig. 5A). MTT results showed that anti-miR-204-5p reversed the proliferation of NOZ and SGC-996 cells inhibited by si-circ_0008234 (Fig. 5B). Also, the EdU positive cells were significantly reduced by si-circ_0008234 in NOZ and SGC-996 cells, while anti-miR-204-5p recovered this effect (Fig. 5C). Moreover, knockdown of circ_0008234 increased the apoptosis rate of NOZ and SGC-996 cells, while miR-204-5p inhibitor down-regulated it (Fig. 5D). Similarly, compared with si-NC, NOZ and SGC-996 cells transfected with si-circ_0008234 showed significantly reduced invasion ability, while anti-miR-204-5p recovered the effect (Fig. 5E). Wound healing assay showed that anti-miR-204-5p reversed the inhibitory effects of circ_0008234 depletion

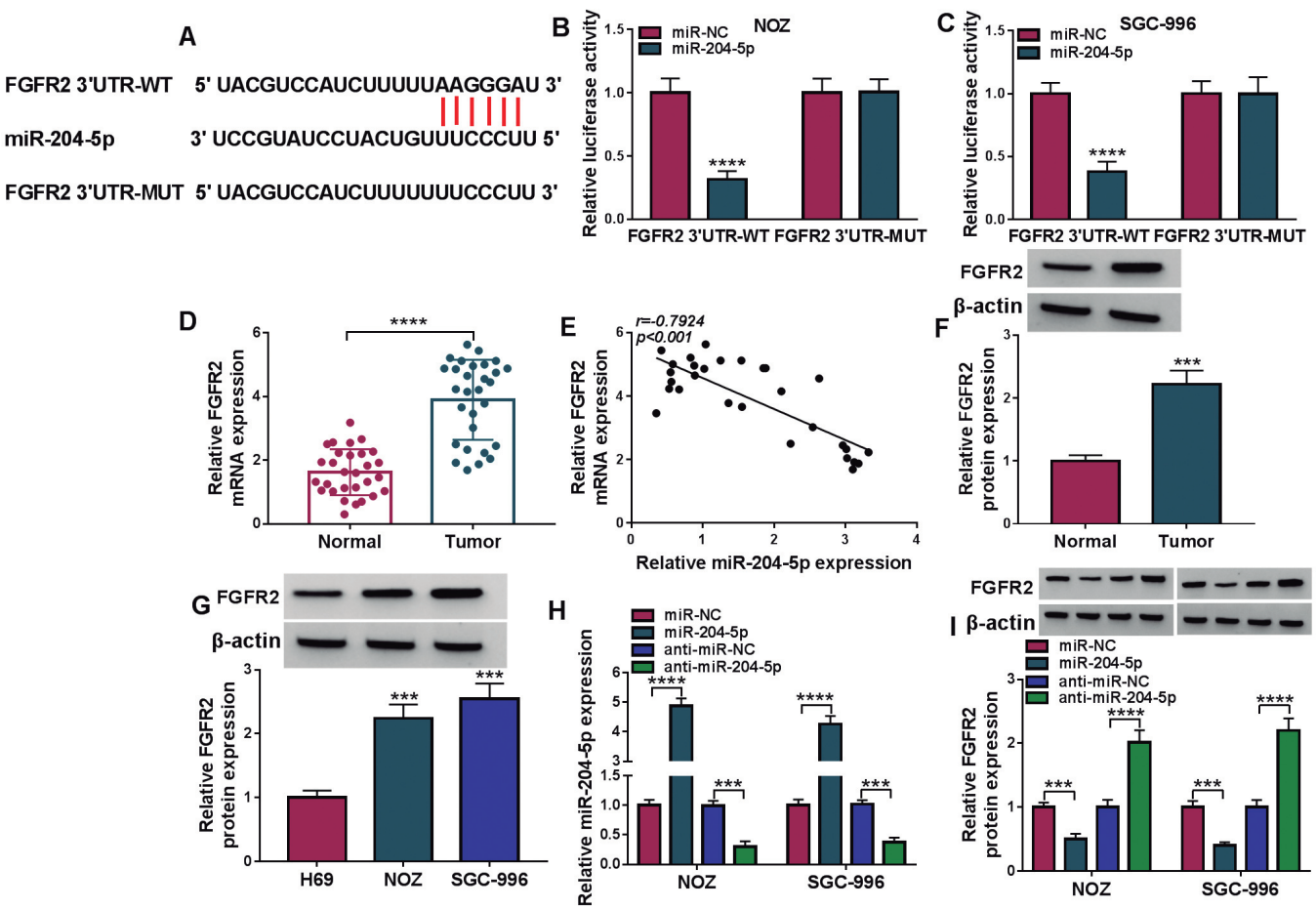

Fig. 6. FGFR2 is a target of miR-204-5p. **A.** Starbase predicted the binding sites of FGFR2 3'UTR to miR-204-5p. **B, C.** Dual-luciferase reporter assays were performed to confirm the association between FGFR2 3'UTR and miR-204-5p. **D.** The expression of FGFR2 in GBC tissues (n=29) was tested by qRT-PCR. **E.** Pearson's correlation analysis. **F, G.** Western blot tested the protein level of FGFR2 in GBC cells. **H.** QRT-PCR detected the expression of miR-204-5p. **I.** Western blot tested the protein level of FGFR2. ****P*<0.001, *****P*<0.0001.

on the migration ability of NOZ and SGC-996 cells (Fig. 5F). Lastly, western blot results showed that the protein levels of CyclinD1 and MMP9 were significantly decreased by decreasing circ_0008234 expression, while, these effects were recovered after transfection with anti-miR-204-5p (Fig. 5G,H). Taken together, miR-204-5p inhibitor reversed the malignant behavior of GBC cells suppressed by circ_0008234 knockdown.

Overexpression of FGFR2 restored the cell behavior affected by overexpression of miR-204-5p in GBC cells

Fig. 6A shows binding sites between FGFR2 3'UTR and miR-204-5p. Dual-luciferase reporter results showed that the combined transfection of miR-204-5p and FGFR2 3'UTR-WT significantly inhibited luciferase activity, while the combined transfection of miR-204-5p and FGFR2 3'UTR-MUT showed no significant change (Fig. 6B,C). Furthermore, the results of qRT-PCR showed that FGFR2 was highly expressed in GBC tissues (Fig. 6D). Pearson's correlation analysis showed that miR-204-5p was negatively regulated with FGFR2 (Fig. 6E). Moreover, we detected the protein level of FGFR2 in GBC tissues and cells, and the results showed that FGFR2 was highly expressed in GBC tissues and cells (Fig. 6F,G). Next, the overexpressed and knockdown efficiency of miR-204-5p were measured by qRT-PCR (Fig. 6H). Western blot confirmed that the expression of FGFR2 was diminished by overexpression of miR-204-5p, and increased by anti-miR-204-5p (Fig. 6I). Furthermore, silencing circ_0008234 significantly reduced FGFR2 expression in NOZ and SGC-996 cells, whereas anti-miR-204-5p partially restored it (Fig. 7A,B), suggesting that circ_0008234 controlled FGFR2 expression through miR-204-5p.

Western blot detected that the overexpressed FGFR2 reversed the expression of FGFR2 inhibited by miR-204-5p (Fig. 8A). Also, MTT results showed that the proliferation of NOZ and SGC-996 cells after transfection with miR-204-5p was significantly decreased, while overexpressed FGFR2 reversed it (Fig. 8B). EdU positive cells were significantly reduced by miR-204-5p in NOZ and SGC-996 cells, while overexpressed FGFR2 reversed it (Fig. 8C). Moreover, miR-204-5p increased the apoptosis rate of NOZ and SGC-996 cells, while the effect was decreased by FGFR2 (Fig. 8D). Moreover, overexpression of FGFR2 recovered the cell invasion and migration ability reduced by miR-204-5p (Fig. 8E,F). Lastly, western blot results showed that overexpressed miR-204-5p decreased the protein levels of CyclinD1 and MMP9, while overexpressed FGFR2 partially reversed them (Fig. 8G,H). In general, miR-204-5p regulated GBC malignant behaviors through interaction with FGFR2.

Knockdown of circ_0008234 inhibited tumor growth in vivo

In order to better study the function of circ_0008234 on GBC, we constructed a xenotransplantation model of GBC. By recording and observing tumor volume (Fig. 9A) and tumor weight (Fig. 9B), we found that knocking down circ_0008234 notably inhibited tumor growth. Then, qRT-PCR detected that the expression of circ_0008234 in the tumor tissues was significantly decreased by sh-circ_0008234, and the expression of miR-204-5p was significantly increased by sh-circ_0008234 (Fig. 9C). Similarly, western blot analysis also confirmed that sh-circ_0008234 significantly reduced FGFR2 protein levels *in vivo* (Fig. 9D). To

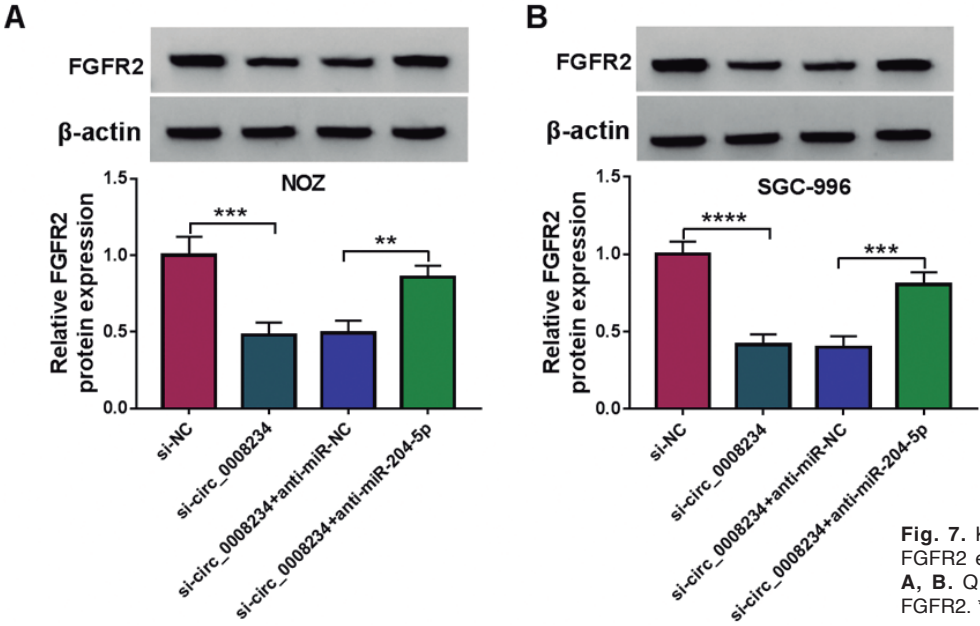

Fig. 7. Knockdown of circ_0008234 inhibited FGFR2 expression by up-regulated miR-204-5p. **A, B.** QRT-PCR detected the expression of FGFR2. ***P*<0.01, ****P*<0.001, *****P*<0.0001.

validate the effect of sh-circ_0008234 on xenograft tumor growth, we performed IHC assay by staining for cell proliferation using the cell-cycle marker Ki67 and found that the sh-circ_0008234 tumors had significantly fewer cells stained for Ki67 than the controls (Fig. 9E), indicating that circ_0008234 knockdown inhibited tumor growth *in vivo*. Finally, IHC results also showed that knocking down circ_0008234 significantly reduced the positive rate of FGFR2 and MMP9 (Fig. 9E), suggesting that circ_0008234 knockdown might affect tumor metastasis. In conclusion, down-regulation of circ_0008234 reduced the tumor development of GBC *in vivo* by the upregulation of miR-204-5p and the reduction of FGFR2.

Discussion

Studies have shown that circRNA, as ceRNA, competes with miRNA to regulate the pathogenesis of cancer by mRNA (Karreth and Pandolfi, 2013). In this study, we suggested that circ_0008234 can act as a therapeutic target for gallbladder carcinoma through miR-204-5p/FGFR2 molecular pathway.

Recently, many studies have reported that circRNAs, play a crucial role in a variety of cancers and tumors (Zhang et al., 2018). For example, circ_0008234 regulated cutaneous squamous cell carcinoma cell function by sponging miR-127-5p (Cai et al., 2022), and circ_0008234 competes with miR-574-5p to regulate

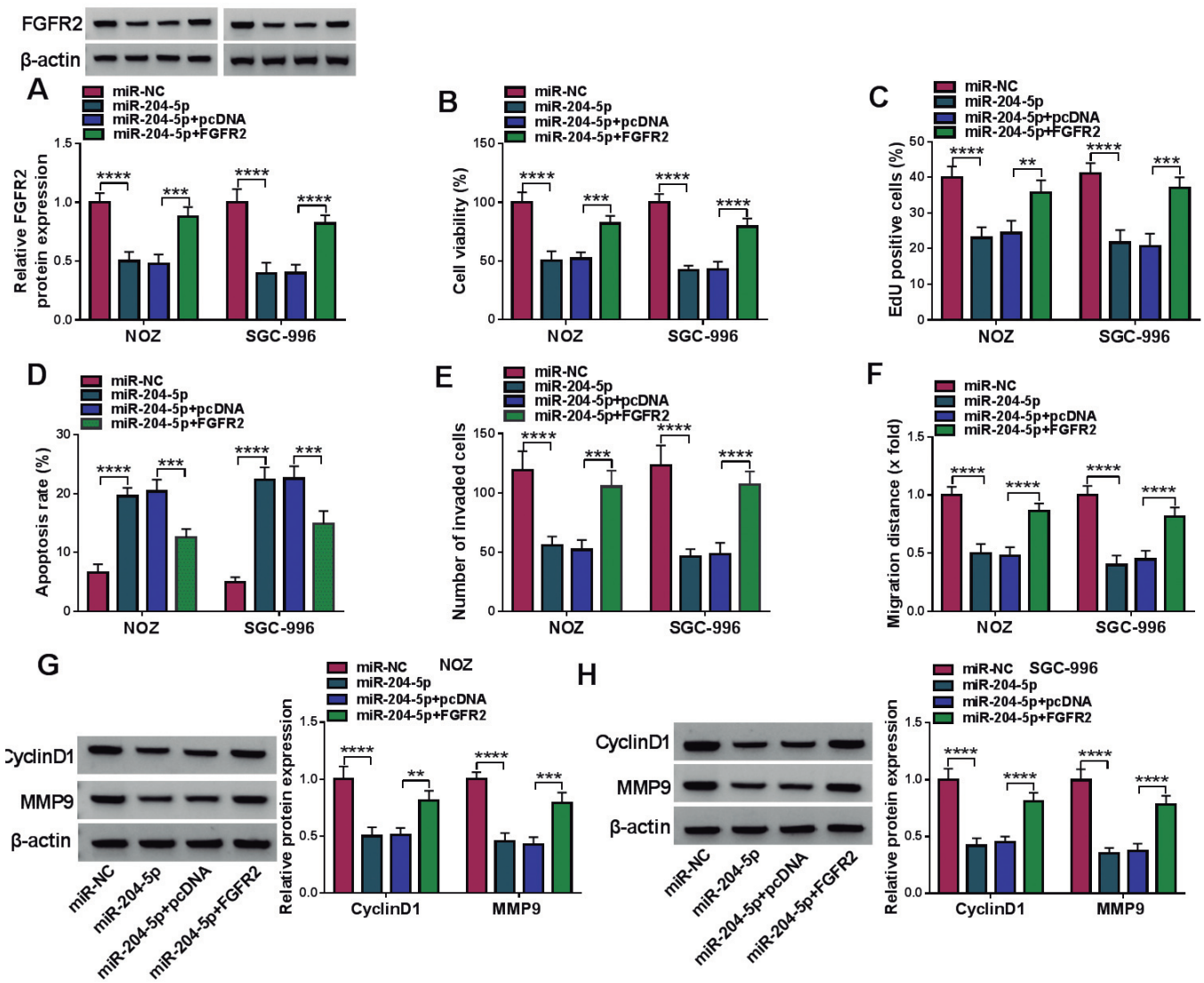

Fig. 8. Overexpression of FGFR2 restored the malignant behaviors reduced by miR-204-5p. **A.** Western blot detected the expression of FGFR2. **B.** MTT detected cell viability. **C.** EdU assay was used to assess EdU positive cells. **D.** Cell apoptosis detected by flow cytometry. **E.** Transwell detected cell invasion ability. **F.** Wound healing assay was used to examine cell migration ability. **G, H.** Western blot assay was used to test the relative protein level. ***P*<0.01, ****P*<0.001, *****P*<0.0001.

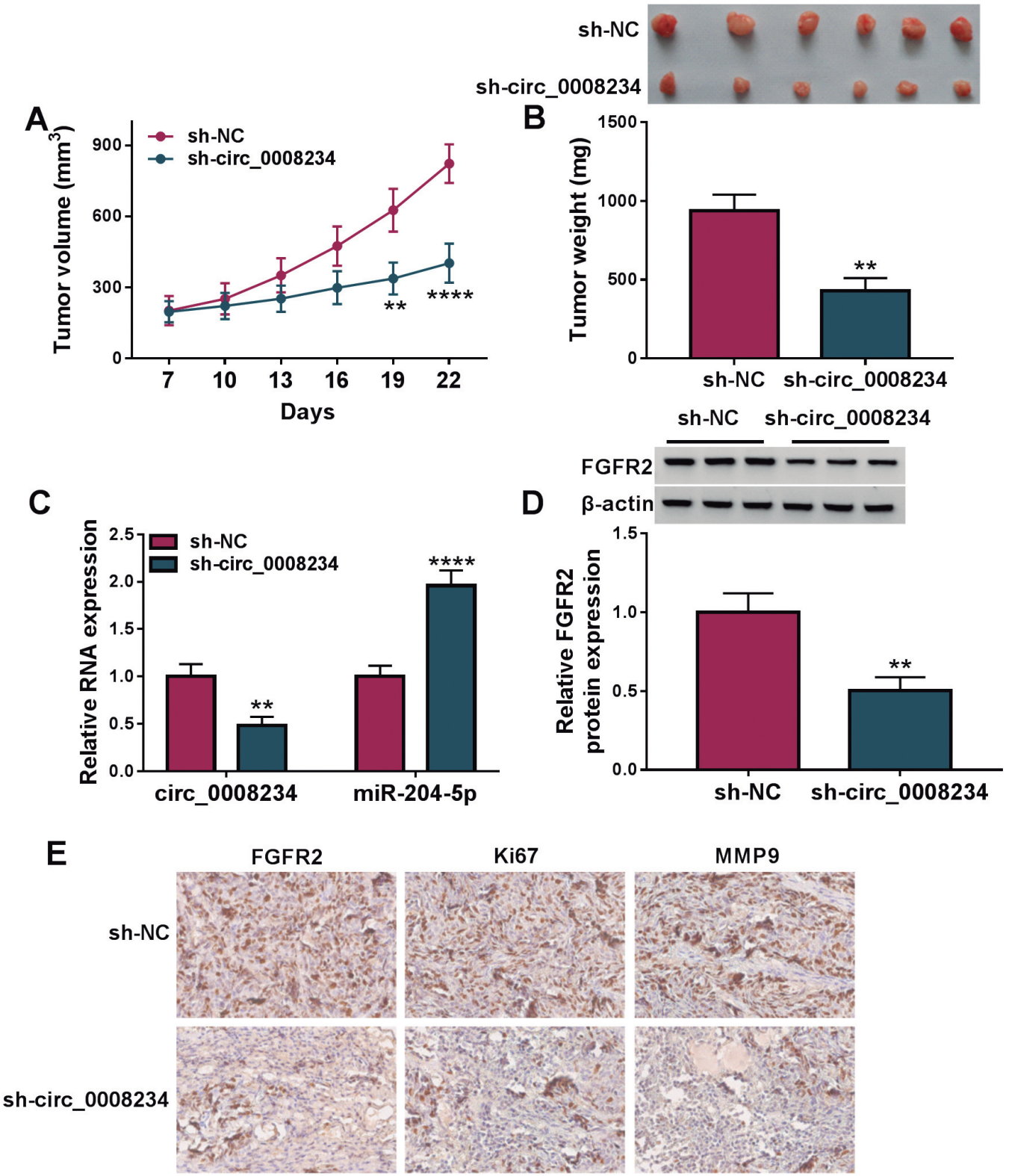

Fig. 9. Circ_0008234 knockdown inhibited tumor growth *in vivo*. **A, B.** Tumor volume and weight after circ_0008234 knockdown *in vivo*. **C.** Relative expression levels of circ_0008234 and miR-204-5p in xenografts were detected by qRT-PCR. **D.** The expression of FGFR2 was analyzed by western blot. **E.** The positive rate of FGFR2, Ki67 and MMP9 was analyzed by IHC. ***P*<0.01, ****P*<0.001, *****P*<0.0001.

lung adenocarcinoma cell growth (Jiang et al., 2021). Similarly, Wang et al. also proved that circ_0008234 was a biomarker in GBC (Wang et al., 2019). We investigated the role of circ_0008234 in GBC, which is consistent with the previous findings of high expression of circ_0008234 in gallbladder carcinoma. Functionally, silencing circ_0008234 inhibited the malignant behavior of GBC cells.

Recent studies have shown that circRNAs sponge miRNAs to mitigate the inhibiting effects of mRNA on cancer (Kulcheski et al., 2016). Moreover, to verify the potential molecular mechanism of circ_0008234 in GBC, we predicted that miR-204-5p was a target of circ_0008234. Fan et al. discovered that circKMT2E suppressed miR-204-5p level to modulate the progress of diabetic cataract (Fan et al., 2019). Huang et al. demonstrated that circ-E2F3 modulated the viability of retinoblastoma cells by targeting miR-204-5p (Huang et al., 2021). Our results demonstrated that miR-204-5p inhibitors can restore the effect of circ_0008234 silencing on the malignant behavior of GBC cells.

Research has reported that FGFR signaling was a pathway for activation of several cancers, and FGFR2, as one of them, has been reported to be an oncogene that regulates the progression of several cancers (Dienstmann et al., 2014). For example, a study by Goyal and his team found that mutations in FGFR2 was able to alter the drug resistance mechanism in intrahepatic cholangiocarcinoma (ICC) (Goyal et al., 2017), and Saborowski et al. also demonstrated that FGFR2 can be used as a biological target to intervene in the prognosis of ICC (Saborowski et al., 2020). Our study showed that FGFR2 was highly expressed in GBC, and miR-204-5p regulated GBC progression by targeting FGFR2. One miRNA can target many target genes and can inhibit their expression in cancer biology. Thus, we speculate that there are many other miR-204-5p target genes that can reverse the effect of miR-204-5p on GBC cell behaviors. Future investigations are warranted in this field.

In, conclusion, our data confirmed that circ_0008234 regulated the progression of GBC by targeting miR-204-5p/FGFR2, which provided a new approach for further study of the pathogenesis of GBC.

Acknowledgements. Not applicable.

Ethics approval and consent to participate. The present study was approved by the ethical review committee of Xiangyang Central Hospital, Affiliated Hospital of Hubei University of Arts and Science. Written informed consent was obtained from all enrolled patients.

Consent for publication. Patients agreed to participate in this work.

Data Availability Statement. The analyzed data sets generated during the present study are available from the corresponding author on reasonable request.

Authors' contribution. All authors made substantial contribution to conception and design, acquisition of the data, or analysis and interpretation of the data; took part in drafting the article or revising it critically for important intellectual content; gave final approval of the revision to be published; and agree to be accountable for all aspects of the work.

Competing interests. The authors declare that they have no competing interests.

Funding. No funding was received for this work.

References

Cai L., Wang Y., Wu J. and Wu G. (2022). Hsa_circ_0008234 facilitates proliferation of cutaneous squamous cell carcinoma through targeting miR-127-5p to regulate ADCY7. Arch. Dermatol. Res. 314, 541-551.

Czaplinska D., Mieczkowski K., Supernat A., Skladanowski A.C., Kordek R., Biernat W., Zaczek A.J., Romanska H.M. and Sadej R. (2016). Interactions between FGFR2 and RSK2-implications for breast cancer prognosis. Tumour Biol. 37, 13721-13731.

Danan M., Schwartz S., Edelheit S. and Sorek R. (2012). Transcriptome-wide discovery of circular RNAs in Archaea. Nucleic Acids Res. 40, 3131-3142.

Dienstmann R., Rodon J., Prat A., Perez-Garcia J., Adamo B., Felip E., Cortes J., Iafrate A.J., Nuciforo P. and Tabernero J. (2014). Genomic aberrations in the FGFR pathway: opportunities for targeted therapies in solid tumors. Ann. Oncol. 25, 552-563.

Fan C., Liu X., Li W., Wang H., Teng Y., Ren J. and Huang Y. (2019). Circular RNA circ KMT2E is up-regulated in diabetic cataract lenses and is associated with miR-204-5p sponge function. Gene 710, 170-177.

Fong Y., Jarnagin W. and Blumgart L.H. (2000). Gallbladder cancer: comparison of patients presenting initially for definitive operation with those presenting after prior noncurative intervention. Ann. Surg. 232, 557-569.

Goyal L., Saha S.K., Liu L.Y., Siravegna G., Leshchiner I., Ahronian L.G., Lennerz J.K., Vu P., Deshpande V., Kambadakone A., Mussolin B., Reyes S., Henderson L., Sun J.E., Van Seventer E.E., Gurski J.M. Jr, Baltschukat S., Schacher-Engstler B., Barys L., Stamm C., Furet P., Ryan D.P., Stone J.R., Iafrate A.J., Getz G., Porta D.G., Tiedt R., Bardelli A., Juric D., Corcoran R.B., Bardeesy N. and Zhu A.X. (2017). Polyclonal secondary FGFR2 mutations drive acquired resistance to FGFR Inhibition in patients with FGFR2 fusion-positive cholangiocarcinoma. Cancer Discov. 7, 252-263.

Hickman L. and Contreras C. (2019). Gallbladder cancer: Diagnosis, surgical management, and adjuvant therapies. Surg. Clin. North Am. 99, 337-355.

Huang Y., Xue B., Pan J. and Shen N. (2021). Circ-E2F3 acts as a ceRNA for miR-204-5p to promote proliferation, metastasis and apoptosis inhibition in retinoblastoma by regulating ROCK1 expression. Exp. Mol. Pathol. 120, 104637.

Jiang W., He Y., Ma Z., Zhang Y., Zhang C., Zheng N. and Tang X. (2021). hsa_circ_0008234 inhibits the progression of lung adenocarcinoma by sponging miR-574-5p. Cell Death Discov. 7, 123.

Karreth F.A. and Pandolfi P.P. (2013). ceRNA cross-talk in cancer: when ce-bling rivalries go awry. Cancer Discov. 3, 1113-1121.

Konstantinidis I.T., Deshpande V., Genevay M., Berger D., Fernandez-del Castillo C., Tanabe K.K., Zheng H., Lauwers G.Y. and Ferrone C.R. (2009). Trends in presentation and survival for gallbladder cancer during a period of more than 4 decades: a single-institution experience. Arch. Surg. 144, 441-447.

Krell R.W. and Wei A.C. (2019). Gallbladder cancer: surgical

management. Chin. Clin. Oncol .8, 36.

Krol J., Loedige I. and Filipowicz W. (2010). The widespread regulation of microRNA biogenesis, function and decay. Nat. Rev. Genet. 11, 597-610.

Kulcheski F.R., Christoff A.P. and Margis R. (2016). Circular RNAs are miRNA sponges and can be used as a new class of biomarker. J. Biotechnol. 238, 42-51.

Li M., Chen W., Zhang H., Zhang Y., Ke F., Wu X., Zhang Y., Weng M., Liu Y. and Gong W. (2016). MiR-31 regulates the cisplatin resistance by targeting Src in gallbladder cancer. Oncotarget 7, 83060-83070.

Li P., Huang T., Zou Q., Liu D., Wang Y., Tan X., Wei Y. and Qiu H. (2019). FGFR2 promotes expression of PD-L1 in colorectal cancer via the JAK/STAT3 signaling pathway. J. Immunol. 202, 3065-3075.

Li X.Y., Tao H., Jin C., Du Z.Y., Liao W.F., Tang Q.J. and Ding K. (2020). Cordycepin inhibits pancreatic cancer cell growth *in vitro* and *in vivo* via targeting FGFR2 and blocking ERK signaling. Chin. J. Nat. Med. 18, 345-355.

Liu J., Liu T., Wang X. and He A. (2017). Circles reshaping the RNA world: from waste to treasure. Mol. Cancer 16, 58.

Melo S.A. and Esteller M. (2014). Disruption of microRNA nuclear transport in human cancer. Semin. Cancer Biol. 27, 46-51.

Narong S. and Leelawat K. (2011). Basic fibroblast growth factor induces cholangiocarcinoma cell migration via activation of the MEK1/2 pathway. Oncol. Lett. 2, 821-825.

Saborowski A., Lehmann U. and Vogel A. (2020). FGFR inhibitors in cholangiocarcinoma: what's now and what's next? Ther. Adv. Med. Oncol. 12, 1758835920953293.

Sharma A., Sharma K.L., Gupta A., Yadav A. and Kumar A. (2017). Gallbladder cancer epidemiology, pathogenesis and molecular genetics: Recent update. World J. Gastroenterol. 23, 3978-3998.

Wang S., Zhang Y., Cai Q., Ma M., Jin L.Y., Weng M., Zhou D., Tang Z., Wang J.D. and Quan Z. (2019). Circular RNA FOXP1 promotes tumor progression and Warburg effect in gallbladder cancer by regulating PKLR expression. Mol. Cancer 18, 145.

Wang X., Lin Y.K., Lu Z.L. and Li J. (2020). Circular RNA circ-MTO1 serves as a novel potential diagnostic and prognostic biomarker for gallbladder cancer. Eur. Rev. Med. Pharmacol. Sci. 24, 8359-8366.

Yu J., Zhang W., Lu B., Qian H., Tang H., Zhu Z., Yuan X. and Ren P. (2018). miR-433 accelerates acquired chemoresistance of gallbladder cancer cells by targeting cyclin M. Oncol. Lett. 15, 3305-3312.

Zhan M., Zhao X., Wang H., Chen W., Xu S., Wang W., Shen H., Huang S. and Wang J. (2016). miR-145 sensitizes gallbladder cancer to cisplatin by regulating multidrug resistance associated protein 1. Tumour Biol. 37, 10553-10562.

Zhang H.D., Jiang L.H., Sun D.W., Hou J.C. and Ji Z.L. (2018). CircRNA: a novel type of biomarker for cancer. Breast Cancer 25, 1-7.

Zhang B., Cui H., Sun, Y. Wang X., Jia Q., Li J., Yin Y., Sun X., Xu H., Li H., Xu F. and Rong J. (2021). Up-regulation of miR-204 inhibits proliferation, invasion and apoptosis of gallbladder cancer cells by targeting Notch2. Aging (Albany NY) 13, 2941-2958.

Accepted October 24, 2022